Atmos. Meas. Tech., 9, 263–280, 2016
www.atmos-meas-tech.net/9/263/2016/
doi:10.5194/amt-9-263-2016

Atmospheric Measurement Techniques
Open Access
EGU

Real-time analysis of δ^{13}C- and δD-CH_4 in ambient air with laser spectroscopy: method development and first intercomparison results

S. Eyer[1], B. Tuzson[1], M. E. Popa[2], C. van der Veen[2], T. Röckmann[2], M. Rothe[3], W. A. Brand[3], R. Fisher[4], D. Lowry[4], E. G. Nisbet[4], M. S. Brennwald[5], E. Harris[1], C. Zellweger[1], L. Emmenegger[1], H. Fischer[6], and J. Mohn[1]

[1]Empa, Laboratory for Air Pollution & Environmental Technology, Dübendorf, Switzerland
[2]Utrecht University (UU), Institute for Marine and Atmospheric research Utrecht (IMAU), Utrecht, the Netherlands
[3]Max Planck Institute (MPI) for Biogeochemistry, Jena, Germany
[4]Royal Holloway University of London (RHUL), Department of Earth Sciences, Egham, UK
[5]Eawag, Water Resources and Drinking Water, Dübendorf, Switzerland
[6]University of Bern, Climate and Environmental Physics, Bern, Switzerland

Correspondence to: J. Mohn (joachim.mohn@empa.ch)

Received: 30 June 2015 – Published in Atmos. Meas. Tech. Discuss.: 31 August 2015
Revised: 6 January 2016 – Accepted: 13 January 2016 – Published: 27 January 2016

Abstract. In situ and simultaneous measurement of the three most abundant isotopologues of methane using mid-infrared laser absorption spectroscopy is demonstrated. A field-deployable, autonomous platform is realized by coupling a compact quantum cascade laser absorption spectrometer (QCLAS) to a preconcentration unit, called trace gas extractor (TREX). This unit enhances CH_4 mole fractions by a factor of up to 500 above ambient levels and quantitatively separates interfering trace gases such as N_2O and CO_2. The analytical precision of the QCLAS isotope measurement on the preconcentrated (750 ppm, parts-per-million, µmole mole^{-1}) methane is 0.1 and 0.5 ‰ for δ^{13}C- and δD-CH_4 at 10 min averaging time.

Based on repeated measurements of compressed air during a 2-week intercomparison campaign, the repeatability of the TREX–QCLAS was determined to be 0.19 and 1.9 ‰ for δ^{13}C and δD-CH_4, respectively. In this intercomparison campaign the new in situ technique is compared to isotope-ratio mass spectrometry (IRMS) based on glass flask and bag sampling and real time CH_4 isotope analysis by two commercially available laser spectrometers. Both laser-based analyzers were limited to methane mole fraction and δ^{13}C-CH_4 analysis, and only one of them, a cavity ring down spectrometer, was capable to deliver meaningful data for the isotopic composition. After correcting for scale offsets, the average difference between TREX–QCLAS data and bag/flask sampling–IRMS values are within the extended WMO compatibility goals of 0.2 and 5 ‰ for δ^{13}C- and δD-CH_4, respectively. This also displays the potential to improve the interlaboratory compatibility based on the analysis of a reference air sample with accurately determined isotopic composition.

1 Introduction

Methane (CH_4) is the second most important anthropogenically emitted greenhouse gas after carbon dioxide (CO_2). Its globally averaged mole fraction has increased from around 722 ppb (parts-per-billion, nmole mole^{-1}) in pre-industrial times to 1824 ppb in 2013 and the anthropogenic fraction is estimated to be 60 % of the total emissions (MacFarling Meure et al., 2006; WMO/GAW, 2015). While the tropospheric methane mole fraction and the most important sources, such as wetlands, ruminants, rice agriculture, fossil fuel production, landfills and biomass burning, are relatively well known, considerable uncertainty remains regarding the strength and spatiotemporal variability of individual sources (Ciais et al., 2013; Dlugokencky et al., 2011; Manning et al., 2011; Rigby et al., 2012). A promising approach to improve the understanding of the CH_4 budget is the use of isotopologues to distinguish between various CH_4 source processes (Beck et al., 2012; Bergamaschi et al., 1998a; Fischer et al., 2008; Fisher et al., 2006; Nisbet et al., 2014). The isotopic

composition is reported in the δ-notation, representing the relative difference in the amount of heavy vs. light isotope of a sample in relation to an international measurement standard (Brand and Coplen, 2012; Coplen, 2011; Urey, 1948):

$$\delta^{13}C = R_{\text{sample}}/R_{\text{standard}}, \quad (1)$$

where R represents the ratio $[^{13}CH_4]/[^{12}CH_4]$ in the case of δ^{13}C, and analogously $[CH_3D]/[CH_4]$ for δD. The international isotopic standards are Vienna Pee Dee Belemnite (VPDB) for δ^{13}C and Vienna Standard Mean Ocean Water (VSMOW) for δD (Werner and Brand, 2001). Measuring δ^{13}C- and δD -CH_4 is a great challenge, as the heavy isotopologues have low natural abundance, i.e., 1.1 % for $^{13}CH_4$ and 0.06 % for CH_3D of total CH_4 in the atmosphere. Nevertheless, combining the analysis of the CH_4 mole fraction and its isotopic composition with inverse modelling techniques and chemical transport models has the potential to validate emission scenarios (Monteil et al., 2011). Current modelling efforts, however, are restricted by the limited continuity and temporal resolution of δ^{13}C-CH_4 measurements and the limited availability of δD-CH_4 data (Monteil et al., 2011). This was confirmed by an observing system simulation experiment, which showed significant reduction in the uncertainty of emission estimates from major national and global CH_4 source categories in the case of model-generated availability of real-time high-precision measurements for δ^{13}C- and δD-CH_4 data (Rigby et al., 2012). A critical requirement for such an observing system is the availability of a suitable high-precision measurement technique. Currently, IRMS is the standard technique to perform high-precision analysis of δ^{13}C- and δD-CH_4 in ambient air (Bock et al., 2010, 2014; Brass and Röckmann, 2010; Fischer et al., 2008; Sapart et al., 2012; Schmitt et al., 2014). Being a laboratory-based technique, it relies on flask sampling, which severely limits its temporal and spatial resolution capability. Furthermore, the analysis of both isotope ratios requires two separate instruments with corresponding sample preparation.

Laser spectroscopy in the mid-infrared (MIR) spectral range has emerged as a powerful alternative for the analysis of stable isotopes of CO_2 (Sturm et al., 2013), N_2O (Köster et al., 2013; Mohn et al., 2012) and CH_4 (Bergamaschi et al., 1994, 1998a, b; Santoni et al., 2012). This development has been triggered by the invention and availability of quantum cascade lasers (QCL), which offer high optical power in continuous wave operation at room temperature (Faist, 2006; Faist et al., 2002). This enables the realization of compact, field-deployable instruments for real-time analysis at ppt (parts-per-trillion, pmole mole^{-1}) level precision (Curl et al., 2010; McManus et al., 2010). However, high-precision measurements of low abundance isotopic species of trace gases (such as δD-CH_4) at ambient mole fractions require preconcentration when using direct absorption techniques (Bergamaschi et al., 1998a). The strategy of trace gas preconcentration prior to isotopic analysis by quantum cascade laser spectroscopy (QCLAS) has been demonstrated for nitrous oxide (N_2O) isotopologues (Mohn et al., 2010, 2012) and was applied in an extended field campaign (Wolf et al., 2015).

In this paper, we present further improvements of coupling a preconcentration unit (trace gas extractor, TREX) to QCLAS to achieve real-time, high-precision measurements of methane isotopic composition (δ^{13}C-CH_4, δD-CH_4) in ambient air. We provide details on the preconcentration with TREX and present results of CH_4 isotopologues analysis with QCLAS. The potential of the TREX–QCLAS technique to trace changes in ambient CH_4 isotopic composition was further demonstrated in an interlaboratory comparison campaign. Results are discussed with respect to the scientifically desirable level of compatibility between laboratories for future applications on both near-source studies and measurements of unpolluted air (WMO/GAW, 2013). Additionally, the need for whole air isotopologue reference gases with well-calibrated CH_4 mole fraction and isotopic composition to improve compatibility of measurements performed in different laboratories is discussed.

2 Experimental

2.1 Preconcentration and analysis of CH_4 isotopologues by TREX–QCLAS

2.1.1 Requirements for the preconcentration system

The main analytical challenge in the present work is the quantification of the CH_3D isotopologue considering its very low natural abundance. A further constraint is given by the spectroscopic setup, as the same optical platform is used for simultaneous measurements of the $^{12}CH_4$, $^{13}CH_4$ and CH_3D isotopologues. This unavoidably involves compromises regarding the spectroscopic configuration, in particular the selected optical path length and the amount of trace gas needed to achieve the necessary measurement precision for both isotope ratios. Simulation of CH_4 absorption spectra in the target spectral regions indicated that optimal conditions are realized at a sample gas pressure in the range of 20 to 60 hPa and for mole fractions ranging from 600 up to 1000 ppm CH_4. Since the CH_4 mole fraction in ambient air is generally in the order of 1.8 ppm, the TREX system had to be designed to selectively extract CH_4 from several liter of ambient air and concentrate into a gas volume of around 20 mL (e.g., equivalent to the amount of gas in the 0.5 L absorption cell of the laser spectrometer at a pressure of 40 hPa). In order to fulfill the above requirements, significant developments and innovative solutions for both TREX and QCLAS have been accomplished.

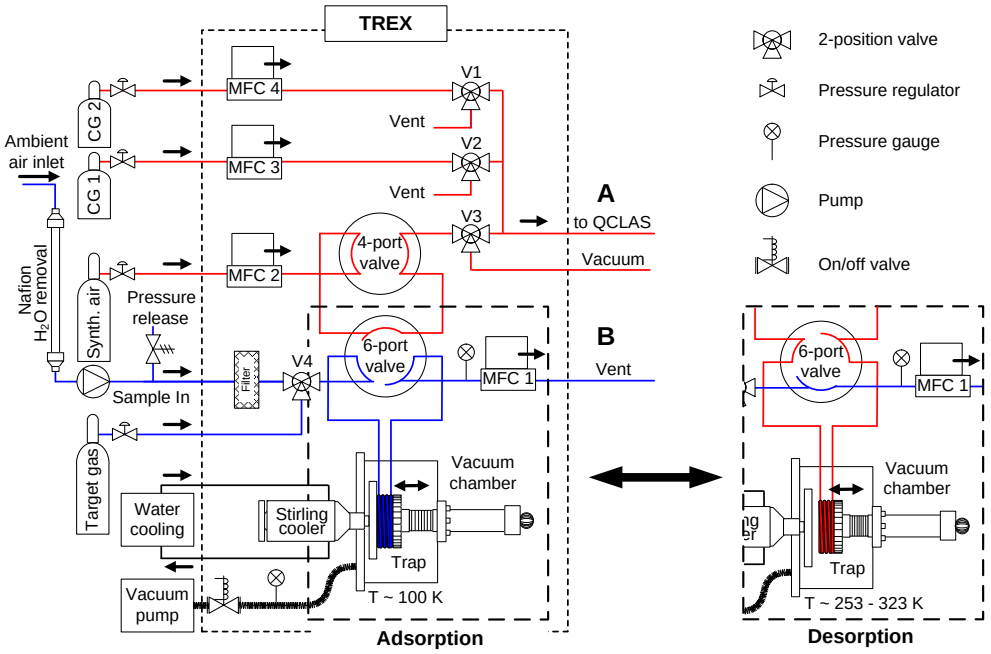

Figure 1. Schematics of the preconcentration unit (TREX). The blue lines indicate the flow of sample air and TG, i.e., ambient air CH_4-mole fractions, while red lines represent the flow of calibration gases and desorbed air, i.e., high CH_4-mole fraction. MFC 1–4 and V1–4 stand for mass flow controllers and 2-position valves, respectively.

2.1.2 TREX: design

The basic technology of the TREX (Fig. 1) is based on the "Medusa" system (Miller et al., 2008), which was later adopted for the preconcentration of N_2O and its subsequent isotope analysis by QCLAS (Mohn et al., 2010, 2012, 2013, 2014; Waechter et al., 2008; Wolf et al., 2015). The main advantages over previously developed systems (Brand, 1995) are the low trapping temperatures in combination with its independence from liquid nitrogen. Preconcentration is achieved by temperature swing adsorption on a cold trap, filled with a specific adsorbent material. The trap is first cooled down to a temperature at which its dynamic adsorbing capacity for the target substance (here CH_4) is sufficiently large, while the majority of the remaining bulk gases (e.g., N_2, O_2, Ar) pass through. During desorption, the trap is heated stepwise to separate the target substance from co-adsorbed interfering compounds. To minimize kinetic fractionation effects, it is important to adsorb and desorb the target substance quantitatively, i.e., with nearly 100 % recovery and with a high degree of reproducibility, as discussed below.

Given the low boiling point temperature of CH_4 (112 K) as an indication for its volatility, the original design of the preconcentration system required major revisions in terms of cooling power to enhance its CH_4 adsorption capacity. In addition, the layout was designed to fit in a compact and field-deployable 19″ rack system. These two requirements led to a novel approach for the trap assembly.

Empirical investigations on the previous preconcentration unit (Mohn et al., 2010) with various trap models adsorbing CH_4 at different temperatures showed that for a complete and reliable CH_4 recovery, the amount of adsorbent material (HayeSep D, Sigma Aldrich, Switzerland) had to be increased by 10-fold. This resulted in 1.8 g of HayeSep D filled in a stainless steel tubing (length 90 cm, OD 4 mm, wall thickness 0.5 mm, volume 6.4 cm^3) and bracketed with glass wool (BGB Analytics AG, Switzerland) and wired mesh. HayeSep D has previously been identified as an excellent high capacity adsorbent material for CH_4 (Eyer et al., 2014). The tubing is curled around a custom-made cylindrical aluminum standoff (outer diameter 70 mm, height 28 mm) with an optimized wall thickness of 0.5 mm. A thermal conductance paste (340 HSC, Dow Corning Inc., USA) is applied at the contact region between trap and standoff to improve heat dissipation. To further increase the adsorption capacity of the trap, the trap temperature had to be decreased to 100 K, which was not achievable with the previous preconcentration unit. Therefore, we decided for a compact Stirling cryo-cooler with a cooling capacity of > 20 W at 100 K (CryoTel GT, Sunpower Inc., USA) gaining in terms of size, weight and cooling performance, with respect to the standard refrigeration unit (PCC: Polycold Compact Cooler, Brooks Automation, USA) employed in the Medusa preconcentration device (Miller et al., 2008). A copper plate disk (diameter 14 cm, weight 1.4 kg) was mounted on the cold tip of the cooler, serving as a cold plate with large heat capacity. Furthermore, we minimized the thermal cycle time of

the trap for repeated adsorption/desorption processes through a design in which the trap is movable by a linear actuator (ZLD225MM, VG Scienta Ltd, UK). During cooling, the actuator pushes the aluminum standoff against the cold plate. The contact pressure is adjusted to 100 N using a chromium-steel corrugated spring (WF-8941-SS, Durovis AG, Switzerland) placed centrically between actuator and standoff. The flat bottom surface of the aluminum standoff and the copper cold plate were polished and coated with a thin layer of heat conductance paste (340 HSC, Dow Corning Inc., USA) to improve thermal contact. Before heating, the standoff is decoupled from the cold plate. This approach is overall faster and yields lower trap temperatures compared to the previous preconcentration unit because the cold plate and the Stirling cooler are completely undisturbed during the heating process.

For thermal isolation of the system, the core parts of the unit, i.e., the cold tip of the Stirling cooler, the cold plate and the trap are housed in a custom-made vacuum chamber evacuated to $< 10^{-4}$ mbar with a compact turbomolecular pump station (HiCube 80 Eco, Pfeiffer Vacuum GmbH, Switzerland). The TREX unit is controlled and monitored by a custom-developed LabVIEW program (National Instruments Corp., USA) with a graphical user interface. All peripherals are connected through a 16-port serial-to-ethernet connector (Etherlite 160, Digi International Inc., USA).

2.1.3 TREX: preconcentration procedure

The overall CH_4-preconcentration cycle can be divided into three main phases, as illustrated by Fig. 2: CH4-adsorption (phase I, 25 min), CH4-desorption (phase II, 15 min) and trap conditioning (phase III, 5 min). At the onset of phase I, the trap is brought in contact with the cold plate by the actuator. It takes about 15 min for the trap to cool down to a temperature of 101 K, then CH_4 adsorption is initiated by switching the six-port multi-position rotary valve (Valco Instruments Inc., Switzerland) to the adsorption position as shown in Fig. 2. Dehumidified (nafion drier with dew point < 230 K, PD-50T-72MSS, Perma Pure, USA), particle-filtered (2-micron filter, SS-4FW-2, Swagelok, Switzerland) sample gas is pushed through the cooled trap with a membrane pump (PM 25032-022, KNF, Switzerland) at a pressure of 4000 hPa. The sample gas flow is adjusted downstream of the trap to a flow rate of 900 mL min^{-1} using a mass flow controller (MFC 1, Vögtlin Instruments, Switzerland). After 500 s, corresponding to preconcentration of 7.5 L sample gas, the six-port rotary valve is switched to the desorption position.

In phase II (CH_4 desorption), the linear actuator decouples the trap from the copper cold plate with the six-port rotary valve set to the desorption position (Fig. 1). Step-wise desorption enables quantitative separation of the target substance CH_4 from more volatile gases (e.g., traces of N_2, O_2) and less volatile trace gases, e.g., CO_2 and N_2O. To avoid

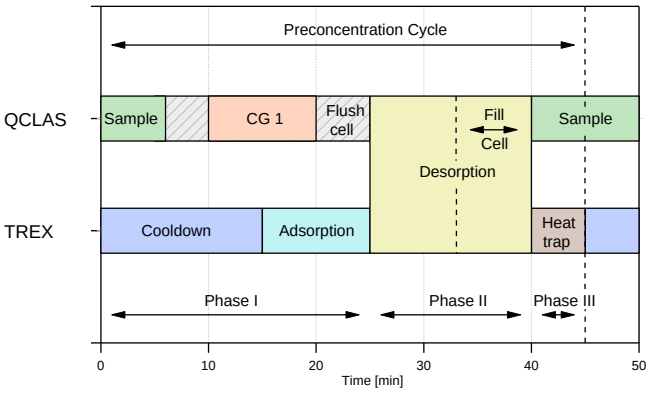

Figure 2. Workflow of QCLAS (top) and TREX (bottom) during a complete measurement cycle consisting of three phases: CH_4-adsorption (phase I), CH_4-desorption (phase II) and trap conditioning (phase III). During phase I, the sample gas and CG1 are analyzed by QCLAS with intermediate flushing, while the adsorbent trap is cooled down by coupling to the base plate, and CH_4 from ambient air is adsorbed. During phase II, CH_4 desorption is initialized by decoupling the trap from the base plate and sequential heating of the adsorbent trap. In addition, desorbed CH_4 is filled into the QCLAS gas cell. In phase III, the adsorbent trap is conditioned (TREX), while the analysis of the sample gas is initialized (QCLAS).

that the latter gases, which are mainly adsorbed on the front part of the trap, are released when the ends of the trap heat up, the flow direction in the desorption step is forward. The trap temperature during phase II is stepwise increased. Immediately after decoupling, its temperature increases from around 106 to 113 K without heating. Then, the trap temperature is raised first to 145 K and then to 175 K by heating with a round flexible polyimide heat foil (diameter 62.2 mm, 100 W, HK5549, Minco Products Inc., USA) placed centrically at the bottom of the aluminum standoff and controlled by a PID temperature controller (cTron, Jumo Mess- und Regeltechnik AG, Switzerland). During this period, mainly volatile bulk gases (e.g., N_2, O_2, Ar) with low boiling points (77 to 90 K) are desorbed from the trap and vented through the QCLAS multipass cell. The CH_4 desorption is initiated by increasing the trap temperature to 258 K and purging with 2 mL min^{-1} high-purity synthetic air (20.5 % O_2 in N_2, purity 99.999 %, Messer Schweiz AG). In parallel, a two-way solenoid valve (series 9, Parker Hannifin Corp., USA) at the outlet of the evacuated QCLAS gas cell is closed; the desorbed methane is thus accumulated in the cell. When the pressure in the QCLAS absorption cell reaches 39.64 ± 0.04 hPa (Baratron 700B, MKS Instruments, USA), the solenoid valve at the inlet of the cell is closed, isolating the desorbed CH_4 in the cell for subsequent analysis.

After CH_4 desorption, phase III (conditioning) is initiated, in which the residual, less volatile trace gases are removed from the HayeSep D trap to assure reproducible starting conditions for each preconcentration cycle. This is achieved by

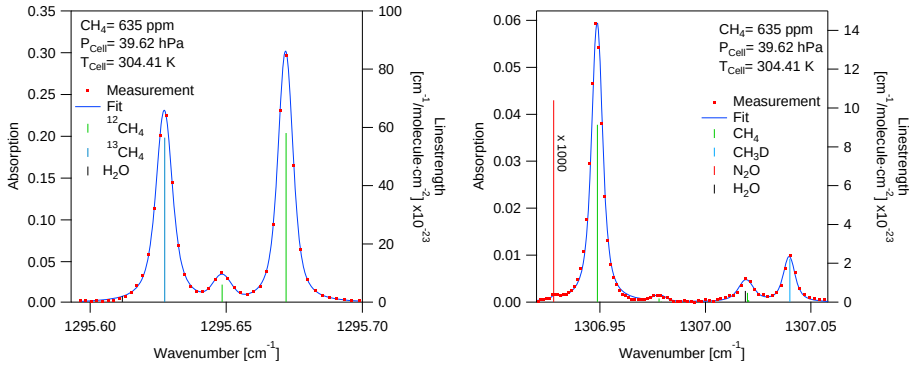

Figure 3. Measured absorption spectra for the determination of δ^{13}C- (left) and δD-CH_4 (right) along with the spectral fit using Voigt profiles and the corresponding line-strengths from the HITRAN database. Potential interferences are expected mainly from N_2O and H_2O. The spectral line of N_2O is divided by a factor of 1000 to fit in the graph, evidencing that even N_2O-mole fraction of around 300 ppb can cause severe interference.

heating the trap to 323 K and purging it for 5 min at reduced pressure (via V3, N920APE, KNF, Switzerland) with 25 mL min^{-1} high-purity synthetic air in backward flow direction. Thereby, residual gas compounds such as H_2O, N_2O, CO_2 and VOCs are removed. The preconcentration cycle is completed by turning the six-port rotary valve to isolate the HayeSep D trap.

2.1.4 QCLAS

The laser spectrometer is a modified version of a previous dual-QCL instrument (QCL-76-D, Aerodyne Research Inc., USA) with a multi-pass cell of 76 m optical path length and a volume of 0.5 L, originally developed for CH_4, N_2O and NO_2 eddy flux measurements (Tuzson et al., 2010). To comply with the demanding requirements of high-precision isotope ratio measurements, critical elements of the hardware electronics were upgraded as described in the following.

Because laser operation stability is of outmost importance, ultra-low noise laser drivers (QCL1000, Wavelength Electronics Inc., USA) were installed to minimize laser intensity variations and frequency jitter. The long-term performance was improved by tighter and more precise control of the laser heat-sink temperature by deploying high-precision controllers (PTC5K-CH, Wavelength Electronics Inc., USA). A new pair of continuous wave DFB-QCL laser (Alpes Lasers SA, Switzerland) was installed. Figure 3 shows the covered spectral range at wavenumbers of 1295.7 and 1307.0 cm^{-1}, selected for δ^{13}C- and δD-CH_4, respectively. The spectral regions were chosen to offer maximum sensitivity for the less abundant CH_3D isotopologues ($\sim 10^{-22}$ cm^{-1}/(molecule $\times$ cm^{-2})), comparable line-strength for $^{13}CH_4$ and $^{12}CH_4$ to avoid saturation and are relatively free from spectral interferences by other molecular species. The susceptibility to spectral interferences could be further reduced by decreasing the pressure in the laser spectrometer gas cell. These conditions could not be fulfilled within the tuning capabilities of a single DFB-QCL, therefore, the simultaneous measurement of δ^{13}C- and δD-CH_4 required a dual-laser configuration (McManus et al., 2011). The measured absorption spectra were analyzed using commercially available software (TDLWintel, Aerodyne Research Inc., USA). In terms of precision and long-term stability, the instrument performance was characterized using the Allan variance technique (Werle, 2010).

In combination with the TREX technique the laser spectrometer is operated in a batch mode; i.e., the multipass cell is either filled with preconcentrated sample or with calibration gas. Before each preconcentrated sample (ambient or pressurized air), the cell is purged for 2 min with high-purity synthetic air at 25 mL min^{-1} flow rate and reduced pressure (8 hPa) and then evacuated to a pressure of 0.5 hPa. Similarly for the calibration gas measurements, the cell is first purged and then flushed with calibration gas dynamically diluted with high-purity synthetic air to the desired CH_4 concentration at a total gas flow of 25 mL min^{-1}. The cell pressure is set to around 40 hPa ($\pm$0.04 hPa).

2.2 Interlaboratory comparison campaign

The intercomparison campaign took place from 6 to 22 June 2014 at the Empa campus, located in the densely populated area of Dübendorf, Switzerland (47°24′11″ N/8°36′48″ E, elevation 432 m a.s.l.). A main road passes 100 m south and a highway around 750 m north of the sampling site. Air was continuously sampled from the rooftop of a five-story building at a flow rate of 25 L min^{-1} through a 25 m long unheated polyethylene-coated aluminum tubing (ID 9 mm, Synflex-1300) using a piston pump (Gardner Denver Thomas GmbH). At the inlet of the sampling pump the air was branched off to the different analyzers, as indicated in Fig. 4. The purpose of the campaign is to validate the TREX–QCLAS system under unattended operation conditions comparable to a "field

campaign". Flask and bag sampling as well as calibration of the commercial available laser spectrometers, however, were operated manually.

2.2.1 Calibration gases and target gas

The calibration gases CG 1 and CG 2 were prepared at Empa from pure fossil (99.9995 %, Messer, Switzerland) and biogenic CH_4 (> 96 %, biogas plant Volketswil, Switzerland), diluted with high-purity synthetic air. The exact amounts of added CH_4 were determined using a high precision flow measurement device (molbox1, DH Instruments Inc., USA), and the dilution with synthetic air was controlled gravimetrically (ID 3, Mettler Toledo GmbH, Switzerland). Before use, the biogenic CH_4 was purified from major contaminants, mainly CO_2 and H_2O, by flushing it through an Ascarite/$Mg(ClO_4)_2$ trap. The δ^{13}C and δD-CH_4 values of the reference gases CG 1 and CG 2, as well as of a cylinder with pressurized air used as the target gas were calibrated against the calibration scales of the Stable Isotope Laboratory of the Max Planck Institute (MPI) for Biogeochemistry in Jena, Germany (Sperlich et al., 2012, 2013; P. Sperlich, personal communication, 2016). It should be noted that the isotopic composition of the measuring gas is outside the range covered by the calibration gases CG1 and CG2 for δ^{13}C and δD-CH_4, which may create problems for analytical techniques with a non-linear response to isotope ratios. This, however, is assumed to be compensated by a correction of results of all analytical techniques/laboratories for the offset in the target gas between assigned value determined by MPI and respective measured values. Results of all analytical techniques/laboratories were corrected for the offset in the target gas between assigned value determined by MPI and respective measured values.

The CH_4 mole fractions of CG 1 and CG 2 were analyzed with QCLAS against commercial standards for CH_4 mole fractions (1000 ± 20 ppm CH_4 in synthetic air, Messer, Switzerland), while the target gas was analyzed by WCC-Empa against the NOAA/GMD scale by CRDS (G1301, Picarro Inc., USA). Table 1 summarizes the CH_4 mole fractions and δ values of TG, CG 1 and CG 2.

2.2.2 TREX–QCLAS

During the intercomparison campaign a measurement cycle of 220 min duration was applied (Fig. 5), including the measurement of three different types of calibration gases (CG 1 at 635 and 745 ppm, CG 2 at 635 ppm) as well as repeatability measurements with preconcentrated target gas (TG). This sequence allowed the measurement of up to 20 ambient air samples per day.

Raw isotope ratio measurements were at first corrected for their dependence on the laser frequency position followed by a drift correction based on regular measurements of CG 1 at 635 ppm. Calibration factors for referencing isotope ratios

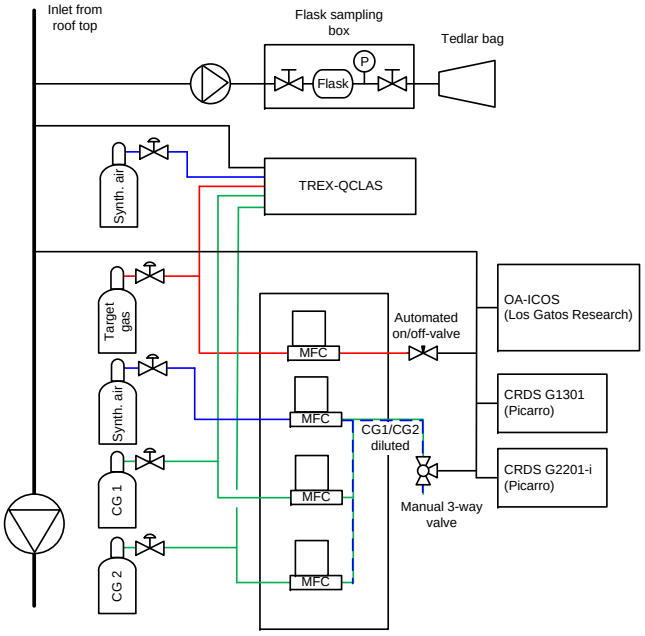

Figure 4. Schematics of the sampling setup used in the interlaboratory comparison campaign. Ambient air was continuously sampled from the rooftop of the building, and split from the main line to the batch sampling unit (bags and flasks), to the TREX–QCLAS system and to the continuous flow CRDS and OA–ICOS spectrometers. The laser spectrometers were additionally supplied with the calibration gases CG 1, CG 2 and the target gas to determine calibration factors and repeatability.

to the international standard scales as well as correction factors to account for the dependence of isotope ratios on CH_4 mole fractions were determined by taking the mean of the calibration gas measurements in intervals of 16 to 48 h and applying a linear regression analysis. Note that the calibration gases were not preconcentrated, thus violating the identical treatment principle. This was compensated, however, by referencing the results to pressurized ambient air (TG) measurements.

The δ^{13}C values of preconcentrated samples were corrected for a 2.3 ‰ offset, which was caused by an increase in O_2 mole fractions to 40 ± 2 % during preconcentration as discussed in Sect. 3.1.2. The δ^{13}C-offset value was shown to be constant for a large range of CH_4 mole fractions and the full range of $\delta-$values covered by this study. For δD-CH_4 no significant effect could be observed; most likely, its magnitude was within the uncertainty of the system.

CH_4 mole fractions in both ambient air and target gas were determined based on the analysis of preconcentrated CH_4 mole fractions ($^{12}CH_4$), divided by the preconcentration factor. This factor was computed for each cycle from the gas volume in the multipass cell and the volume of preconcentrated air. The latter is derived from the sample gas flow and the adsorption time. As the trap additionally adsorbs small amounts of N_2 and O_2 (up to 4 % of the preconcentrated sam-

Table 1. List of CH_4 mole fractions and isotopic composition (δ^{13}C and δD-CH_4) of laboratory standards used in the intercomparison campaign. The indicated uncertainty is the 1 σ standard deviation for repeated analysis of the respective measurement system.

	Composition	CH_4 [ppm]	δ^{13}C-CH_4 [c] [‰]	δD-CH_4 [c] [‰]
CG 1	Fossil/biogenic CH_4 in synthetic air	938.8 ± 3.5[a]	-46.60 ± 0.10	-250.46 ± 1.05
CG 2	Fossil CH_4 in synthetic air	1103.8 ± 3.5[a]	-36.13 ± 0.10	-180.58 ± 1.05
TG	Pressurized ambient air	2.3523 ± 0.0002[b]	-48.07 ± 0.10	-120.00 ± 1.05

CH_4 mole fractions were measured by CRDS [a] after dilution by a factor of 1 : 500 or [b] by direct measurement. [c] Isotopic values were analyzed by IRMS at MPI.

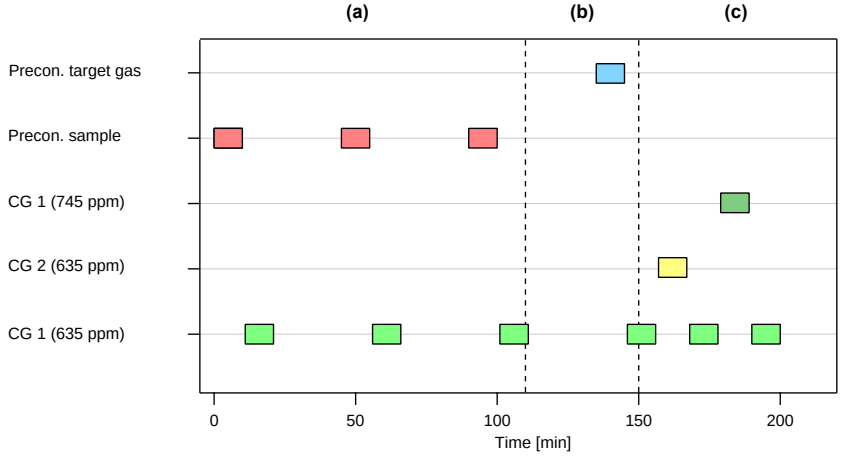

Figure 5. A complete measurement cycle consist of three main sequences: **(a)** three consecutive measurements of preconcentrated discrete ambient air samples, **(b)** one measurement of preconcentrated pressurized air (target gas), followed by the calibration phase **(c)**. The latter is used for the determination of calibration factors for δ^{13}C-CH_4 and δD-CH_4 and the dependence of isotope ratios on elevated CH_4 mole fractions. The calibration gases are dynamically diluted to the indicated CH_4 mole fractions as described in Sect. 2.2.2. All measurements are bracketed by the analysis of CG 1 (anchor) at 635 ppm CH_4 to drift-correct the measurements.

ple volume, depending on the trap temperature), variations in the trap temperature also need to be considered. Finally, the CH_4 mole fraction measurements were linked to the WMO-X2004 calibration scale (Dlugokencky et al., 2005) through calibration of the target gas against NOAA reference standards at Empa.

2.2.3 Commercial laser spectrometers

During the campaign, an off-axis integrated cavity output spectrometer (OA–ICOS, δ^{13}C-CH_4 and CH_4 mole fraction, MCIA-24e-EP, Los Gatos Research, USA) provided by Utrecht University (UU), and a cavity ring-down spectrometer (CRDS, δ^{13}C-CH_4, δ^{13}C-CO_2, CH_4 and CO_2 mole fraction, G2201-I, Picarro Inc., USA) provided by Eawag, were deployed. The OA–ICOS analyzer operated in the MIR spectral region, while the CRDS instrument comprises a NIR laser source. OA–ICOS and the CRDS isotope analyzers were calibrated twice per day using the calibration gases CG 1 and CG 2 (Table 1) for 30 min each. These standards were diluted with high-purity synthetic air by a factor of 1 : 500, to 1955.3 ± 6.8 ppb CH_4, which is close to the ambient mole fraction (Fig. 4). The dependencies of $\delta-$ values on CH_4 mole fraction were linear up to a concentration of around 2500 ppb and determined to be -6.35 and 1.18 ‰ ppm^{-1} for OA–ICOS and CRDS, respectively. Variations over the duration of the campaign were not significant and therefore a constant factor was applied. Thereafter, for both analyzers a drift and a two-point calibration correction for δ^{13}C-CH_4 was performed based on the measurements of CG 1 and CG 2. Finally, 30 min averages of sample data were calculated, resulting in 550 measurement points for the CRDS over the 2-week period of the intercomparison campaign. The repeatability of OA–ICOS and CRDS for δ^{13}C-CH_4 was assessed based on repeated analysis of the target gas (pressurized air) every 6 h for 30 min.

2.2.4 Bag and flask sampling

In addition to the in situ optical analyzers, manual sampling in glass flasks and Tedlar bags for subsequent IRMS laboratory analysis was performed. Glass flasks were purged for 10 min with dehumidified ($Mg(ClO_4)_2$, Sigma-Aldrich, Switzerland) sample gas at 2 L min^{-1} using a membrane pump (KNF, Netherlands) and then filled to 2000 hPa. Air samples collected in glass flasks were analyzed for δ^{13}C-

CH_4, δD-CH_4 and CH_4 mole fraction at the Institute for Marine and Atmospheric research Utrecht (IMAU) of Utrecht University (UU) and a selection of flasks were also analyzed by the Stable Isotope Laboratory of Max Planck Institute (MPI) for Biogeochemistry. Parallel to the glass flask sampling and through the same sample line, 3 L Tedlar bags (SKC Ltd., USA) were filled and subsequently analyzed for δ^{13}C-CH_4 by IRMS and CH_4 mole fraction by CRDS (G1301, Picarro Inc., USA) at the Greenhouse Gas Laboratory, Department of Earth Sciences (GGLES) of the Royal Holloway University of London (RHUL). In total, 81 flask and 48 bag samples were taken at different intervals, usually at least twice per day. Additionally, intensive sampling was performed on 13 June and from 20 June 12:00 to 22 June 12:00 LT (local time), when both flask and bag samples were filled every one to 3 h.

2.2.5 IRMS analysis of δ^{13}C-CH_4 and δD-CH_4 in flask samples at UU

Both δD and δ^{13}C of CH_4 were measured by continuous flow IRMS (Thermo Finnigan Delta plus XL) (Brass and Röckmann, 2010). First a 40 mL stainless steel (SS) sample loop is filled with sample or reference air at atmospheric pressure. The air is flushed by a flow of helium carrier gas (purity 99.9999 %) to the preconcentration unit ($1/8''$ SS tube filled with 6 cm HayeSep D 80–100 mesh) cooled to 137 K, where the CH_4 is retained and separated from the bulk air. The CH_4 is released by heating the adsorbent trap to 238 K and focused on the cryo-focus unit (25 cm PoraPLOT Q, 0.32 mm ID, 117 K). For δD analysis, the CH_4 is injected (by heating the cryo-focus trap to 198 K) into a pyrolysis tube furnace (1620 K), where CH_4 is converted to H_2 and carbon. The H_2 enters the IRMS, after passing a 2 m CarboPLOT column at room temperature (RT) and a nafion dryer, via the GasBench interface. No krypton interference could be determined in this setup. The repeatability for δD-CH_4 is better than $\pm$2 ‰, based on 10 consecutive analyses of standard air. A detailed inter-laboratory comparison between UU and MPI is presently ongoing, and a preliminary scale offset of 4 ‰ has been used for the present evaluation.

For δ^{13}C, the CH_4 is injected from the cryo-focus unit into a combustion oven with nickel wire catalyst at 1373 K, where the CH_4 is converted to CO_2 and H_2O. The resulting gas mixture passes a nafion dryer and a 5 m PoraPLOT Q column (RT) to eliminate an interference from co-trapped krypton (Schmitt et al., 2013) before entering the IRMS via the GasBench interface. The repeatability of δ^{13}C is better than 0.07 ‰.

2.2.6 IRMS analysis of δ^{13}C-CH_4 and δD-CH_4 in flask samples at MPI

At the Stable Isotope Facility of MPI Jena ("BGC-IsoLab") methane isotopes from air samples have been analyzed using a new custom made twin-mass spectrometer analysis system (Delta V+, Thermo-Fisher, Bremen, Germany) with cryogenic preconcentration and GC separation (W. A. Brand, personal communication, 2016). The system allows analyzing δ^{13}C and δD simultaneously in an automated and fully calibrated fashion. For every air sample, a reference air sample is analyzed concurrently. Only the difference between the reference and sample air is used for calibration. While the ion currents are analyzed on the same mass spectrometers, reference and sample air pass through dedicated cryogenic acquisition lines. The isotopic relation between these lines is established daily using four complete analyses with reference air sent through the sample preconcentration duct.

Using small-volume flow controllers, cryogenic acquisition is made at 5 mL min^{-1} over 20 min, thereby consuming 100 mL air for each isotope measurement. Prior to methane concentration, CO_2 is removed cryogenically using a permanent liquid nitrogen bath. The cryo traps for methane retention consist of $1/8''$ stainless steel tubes filled with HayeSep-D polymer for specific absorption of CH_4 at 143 K. The latter temperature is generated by compression coolers (Cryotiger, Brooks Automation, Jena, Germany), which can operate down to 123 K at a heat digestion capacity of around 30 Watt.

After acquisition, the acquired methane is transferred to a cryogenic focus trap of similar design, from where gas chromatographic separation is initiated by rapid heating. The methane peaks are heart cut (Deans, 1968) for combustion (δ^{13}C) and pyrolysis (δD), respectively. CH_4-derived CO_2 is separated from non-reacted CH_4 and from the co-trapped krypton with a post-reaction gas chromatographic separation before being introduced to the respective mass spectrometer via open split coupling. An entire sample carousel with 18 analyses (13 sample analyses net) takes about 27 h.

The system is in continuous operation since July 2012. The overall precision including all instrument failure times is $\pm$0.15 ‰ (δ^{13}C) and $\pm$1.14 ‰ (δD), as determined through daily measurement of a QA (quality assurance) sample air. Removing the times of instrumental malfunction improves the precision to $\pm$0.10 ‰ (δ^{13}C) and $\pm$1.05 ‰ (δD) over the entire period of operation (3 years). The precision for 10 repeated measurements of standard air is typically 0.07 ‰ (δ^{13}C) and 0.7 ‰ (δD).

2.2.7 IRMS analysis of δ^{13}C-CH_4 in bag samples at RHUL

δ^{13}C-CH_4 was measured using a modified GC-IRMS system (Trace Gas and Isoprime, Isoprime Ltd.). This system uses a modified trace gas preparation system in dynamic mode, whereby the original catalyst is replaced by palladized quartz wool in a wider 4 mm ID ceramic furnace tube. Conversion of methane to CO_2 and H_2O is completed at 1063 K using oxygen in the air sample as the oxidant. A highly modified and automated inlet system (Fisher et al., 2006) was ap-

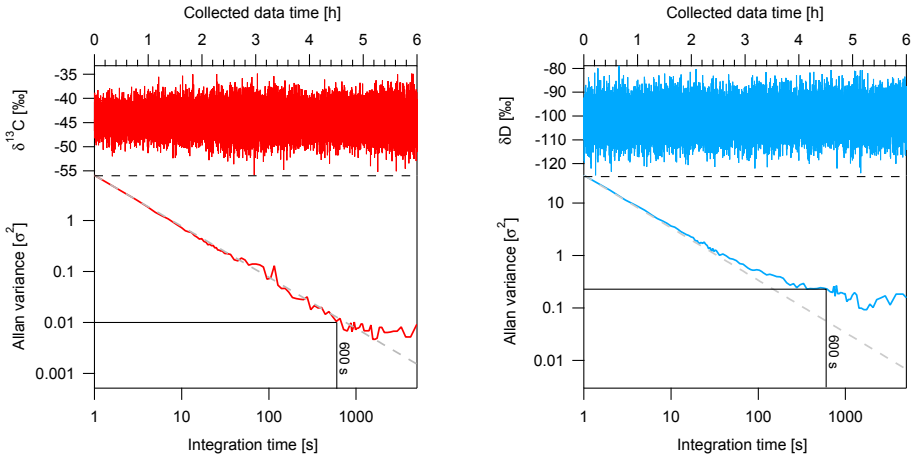

Figure 6. Allan variance plots for δ^{13}C-CH_4 (left) and for δD-CH_3 (right) using 750 ppm CH_4. The upper plot shows the corresponding time series of δ-values recorded at 1 second temporal resolution. At 600 s spectral averaging, the square root of the Allan variance indicates a precision of 0.1 ‰ for δ^{13}C-CH_4 and 0.5 ‰ for δD-CH_4.

plied consisting of an auto-sampler including a six-port rotary valve (Valco Instruments Inc.) with a 75 cm^3 Swagelok stainless steel sample volume and four samples, one standard gas and a vacuum line attached. The 75 cm^3 sample volume is evacuated up to the solenoid valve directly before the bag valve, then the air moves from the bag into the sample volume maintaining ambient atmospheric pressure. This air is then pushed through the preparation system with a flow of helium gas set to a pressure of 758 hPa. Individual sample analysis lasts approximately 19 min and all sample measurements were made in triplicate. Repeatability based on 10 consecutive analyses of standard air is ±0.05 ‰ or better. δ^{13}C-CH_4 values of RHUL are offset corrected by −0.3 ‰ based on intercomparison measurements with NIWA (Lowe et al., 2004).

3 Results and discussion

3.1 TREX–QCLAS

3.1.1 Performance characteristics of QCLAS

The QCLAS precision and stability were investigated using the Allan variance technique. Therefore, individual CH_4 isotopologues were measured with 1 s integration time over a period of a few hours, as shown in Fig. 6. From the associated Allan variance plots, an optimum averaging time of approximately 600 s can be derived, corresponding to a root mean square noise of 0.1 and 0.5 ‰ for δ^{13}C-CH_4 and δD-CH_4, respectively. The 1 s noise performance was determined to be in the $\sim 4.0 \times 10^{-5}$, which corresponds to a noise equivalent absorbance per unit path length of 5.2×10^{-9} cm^{-1} when considering the 76 m optical path.

Similar to earlier work on CO_2 and N_2O (Tuzson et al., 2008; Waechter et al., 2008), we found also in the case of methane a linear dependence of the spectroscopically retrieved isotope ratios on the mole fractions. In a series of experiments, the magnitude of this dependence was empirically determined and verified in the range of 600–1000 ppm CH_4. The coefficients were 0.0145 and −0.0521 ‰ ppm^{-1} for δ^{13}C- and δD-CH_4, respectively. At each calibration phase in the intercomparison campaign, these dependencies were determined repeatedly via two-point calibration and remained stable during the 2-week period.

The influence of laser temperature variation on δ^{13}C and δD values has been determined by systematically changing the laser heat-sink temperature over ± 20 mK in steps of 3 mK, and measuring the changes observed in the retrieved isotope ratios. We found a rather strong linear dependence, i.e., 0.1 and −0.2 ‰ mK^{-1} for δ^{13}C- and δD-CH_4, respectively. Thus, it was crucial not only to control the laser temperature at high-precision (≈ 1 mK), but also to record the laser temperature at high resolution and to apply a drift correction caused by this effect during data post-processing.

3.1.2 Optimization of TREX–QCLAS

The preconcentration procedure was optimized to reduce cycle time and reach the target sample volume of 7.5 L of ambient air, but also to allow quantitative and reproducible CH_4 desorption (> 99.9 %) with simultaneous separation of other trace gases, such as N_2O, CO_2 and H_2O. Various trap temperatures (108 to 93 K) and gas flows (500 to 1000 mL min^{-1}) have extensively been tested and the optimal conditions were found to be 900 mL min^{-1} with an initial trap temperature of 101 K. Under standard operation conditions, the breakthrough volume was determined to be above 9 L of air. During this period, the CH_4 mole fraction downstream of the trap, at the outlet of MFC 1, was below 0.5 ppb (G1301, Picarro Inc., USA). Tests with higher trap temperatures (111 K)

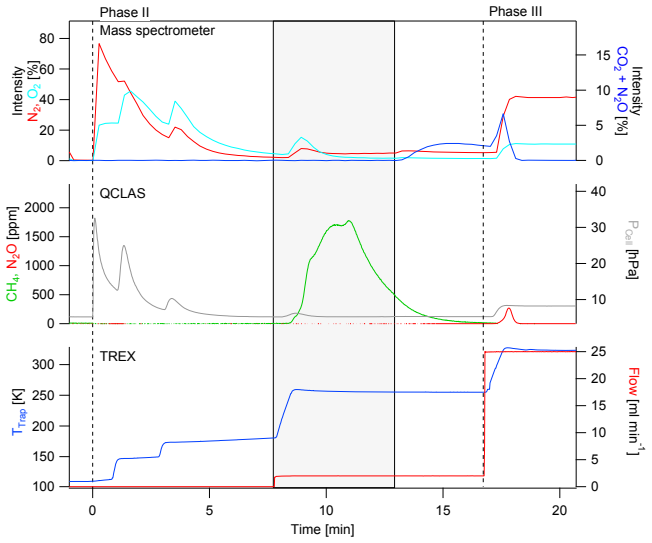

Figure 7. Phase II (desorption) and phase III (conditioning) of the CH_4 preconcentration cycle by TREX. Mass spectrometer results (upper graph) indicate that the bulk gases N_2 and O_2 leave the trap shortly after decoupling the trap from the cold plate and heating successively to 145 K (1 min) and 175 K (3 min), but a small residual is also released in the main CH_4 desorption step (see text for details). QCLAS measurements (middle graph) display that CH_4 desorption is initiated by heating the trap to 258 K (8 min) and purging it with 2 mL min^{-1} synthetic air in forward flow direction; the gray shaded area indicates the period, during which the desorbed methane is filled into the gas cell of the laser spectrometer. In phase III (conditioning) the trap is heated up to 323 K and purged with 25 mL min^{-1} of high-purity synthetic air. The bottom graph exhibits the trap temperatures and flows of synthetic air in the preconcentration device (TREX).

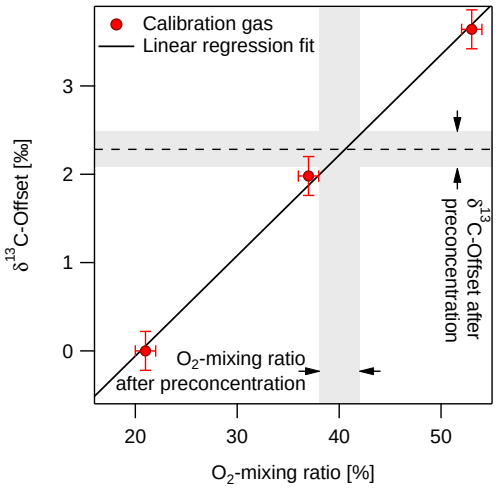

Figure 8. δ^{13}C-offset as a function of O_2 mole fraction determined from measurements of calibration gases without preconcentration with the QCLAS. This effect was found to be constant for CH_4-mole fractions from 600 to 1000 ppm. The grayed region shows the ranges of the O_2-mole fractions in the QCLAS-cell after preconcentration and the resulting offset in the δ^{13}C-values for typical TREX operation as determined from a series of experiments. The dashed horizontal line represents the offset in δ^{13}C values of 2.3 ‰ used as a correction throughout the measurement campaign.

indicated considerable CH_4 breakthrough at much lower adsorption volumes of 6.1 L, given the very high flow rates of 900 mL min^{-1} (data not shown).

Figure 7 displays the sequential desorption of the various compounds adsorbed on the trap. For the optimization of this procedure CH_4 and N_2O were quantified by QCLAS, while N_2, O_2 and CO_2 were measured by a quadrupole mass spectrometer (MKS, Switzerland). Quantitative (> 99.9 %) CH_4 desorption was verified by a subsequent second desorption and analysis of the resulting effluent gas for CH_4. This verifies that the tail in CH_4 mole fractions after the main desorption peak originates from a consecutive flushing of the QCLAS gas cell and not from CH_4 eluting from the trap. In parallel to CH_4, also bulk air components such as O_2 and N_2 are co-desorbed from the trap. Due to the much lower boiling point of O_2 (90 K) relative to N_2 (77 K), the O_2 mixing ratio in the absorption cell after preconcentration is increased to 40 ± 2%. To investigate the effect of this gas matrix change on the δ values and additional fractionation effects, calibration gases with δ^{13}C- and δD-CH_4-values ranging from -36.1 to -58.5 ‰ and -181 to -331 ‰ , respectively, were diluted with synthetic air to mole fractions of 2 and 2.2 ppm CH_4, then preconcentrated and measured against the respective undiluted calibration gas. We observed a constant offset of 2.3 ± 0.2 ‰ for δ^{13}C compared to the undiluted calibration gas, independent of CH_4 mole fraction or δ value. For δD no detectable influence was observed. The most plausible explanation for this effect is a change in the pressure broadening of the line profiles caused by the increased O_2-mixing ratio after preconcentration. The HITRAN database contains the air pressure broadening coefficients only. Consequently, any deviation in the N_2 / O_2 ratio leads to a bias due to this effect, as the fitting model uses improper coefficients for line profile estimation.

In order to verify this hypothesis, we deliberately changed the gas matrix composition by setting its O_2-mole fraction to 21, 37 and 53 %. For each O_2-mixing ratio the CH_4 mole fraction was increased stepwise from 600 to 1000 ppm and the δ^{13}C dependence on CH_4 mole fraction was accounted for. Figure 8 shows the measured dependence of δ^{13}C-CH_4 on changing O_2-mixing ratio. The gray bars indicate the ranges of the O_2-mixing ratio of sample gas after preconcentration as determined by mass spectrometry and the resulting offset in the δ^{13}C-values obtained for individual experiments. As mentioned before, the δD-CH_4 values showed no significant dependence on O_2-mixing ratio.

This result confirms that the O_2 interference is the main source of systematic bias for δ^{13}C-CH_4, whereas fractionation effects for both, δ^{13}C- and δD-CH_4 values, are insignif-

icant. The gas matrix effect could be reduced or at least kept stable by enhancing the temperature control of the trap to constrain the O_2-mixing ratio in the gas matrix and thereby improving the repeatability of δ^{13}C measurements. Another solution could be to substitute the HayeSep D adsorbent material by a candidate either exhibiting a superior selectivity for CH_4 over O_2 or having a larger capacity for CH_4, so that the adsorption temperature can be increased. Higher adsorption temperatures would reduce the amount of O_2 trapped in the system.

3.2 Repeatability of analytical techniques and scale differences between laboratories

Scale differences between different analytical techniques/laboratories and their repeatability were assessed based on repeated target gas measurements (Table 2). Figure 9 shows the histograms of the target gas measurements obtained with the TREX–QCLAS: CH_4 mole fraction of 2352.0 ± 4.4 ppb, δ^{13}C-$CH_4 = -47.99 \pm 0.19$ ‰ and δD-$CH_4 = -120.9 \pm 1.9$ ‰. The repeatability of TREX–QCLAS was comparable to manual sampling with subsequent IRMS analysis for δD-CH_4, but about a factor of 3 worse for δ^{13}C-CH_4. The CRDS exhibited a comparable repeatability (0.24 ‰) to TREX–QCLAS for δ^{13}C-CH_4, while with 0.78 ‰ the performance of OA–ICOS was significantly worse. In summary, the repeatability of TREX–QCLAS, CRDS and all IRMS laboratories offer the capability to reach the extended WMO/GAW compatibility goals for δ^{13}C and δD-CH_4, of 0.2 and 5 ‰, defined for regional scale studies (WMO/GAW, 2013), while the goals for background measuring stations of 0.02 and 1 ‰ for δ^{13}C and δD-CH_4 are beyond the performance of any of the applied techniques. A more detailed discussion is given in Sect. 3.4.

For assessing the compatibility between the instruments, IRMS measurements of MPI were chosen as the reference point, as MPI recently established a direct link to the international isotope standard scales. The data obtained from the laser spectroscopic techniques (TREX–QCLAS, CRDS and OA–ICOS) are referenced to the standards CG 1 and CG 2, analyzed by MPI, while the IRMS measurements of UU and RHUL are referenced to their respective laboratory standards. The agreement for δ^{13}C-CH_4 is within 0.1 ‰ for all techniques/laboratories, except the IRMS measurements of RHUL, which were 0.25 ‰ higher and the OA–ICOS results, which were offset by as much as -8.87 ‰. For δD-CH_4, no significant differences were observed between TREX–QCLAS and the MPI IRMS, while the UU IRMS values were 2.3 ‰ higher.

The ambient air measurements during the campaign were offset-corrected for differences in δ^{13}C and δD-CH_4 measurements of TG by individual techniques/laboratories and MPI summarized in Table 2. Differences for IRMS laboratories include differences in scales and instrumental issues,

Table 2. List of measured δ^{13}C-CH_4 and δD-CH_4 values of the target gas (pressurized air) as reported by different analytical techniques/laboratories. The indicated uncertainty is the 1σ standard deviation. Results of laser spectroscopic techniques are referenced to standards CG 1 and CG 2, while IRMS results where referenced to their respective laboratory standards.

	Number of measurements	δ^{13}C-CH_4 [‰]	δD-CH_4 [‰]
Glass-flask/IRMS (MPI)	1	-48.07 ± 0.10	-120.0 ± 1.05
TREX–QCLAS (Empa)	62	-47.99 ± 0.19	-120.9 ± 1.9
Glass-flask/IRMS (UU)	4	-47.96 ± 0.08	-117.7 ± 2.0
CRDS (Eawag)	64	-48.04 ± 0.24	n.a.
OA–ICOS (UU)	10	-56.94 ± 0.78	n.a.
Bag/IRMS (RHUL)	3	-47.82 ± 0.05	n.a.

n.a.: not analyzed

while the laser spectroscopic techniques are all calibrated using CG 1 and CG 2. The OA–ICOS data are not considered further due to the limited performance with respect to repeatability and scale offset.

3.3 Real-time analysis of CH_4 isotopic composition in ambient air

The CH_4 mole fraction and isotopic composition measurements in ambient air between 6 and 22 June 2014 of the various laser spectroscopic and mass spectrometric analytical techniques is shown in Fig. 10. Data of all laboratories have been offset corrected as discussed in the previous section. During the campaign, more than 250 air samples (199 samples of ambient air, 62 target gas samples) were analyzed in stand-alone operation by TREX–QCLAS and more than 120 manually taken samples were analyzed by IRMS. The CRDS data were averaged for 30 min, resulting in 550 mean values.

The CH_4 mole fractions exhibit a regular diurnal variation with nighttime values increasing up to 2300 ppb, which is around 400 ppb higher than at daytime. When comparing the measurement data from the local weather station in Dübendorf with the measured CH_4-mole fractions, the nights with the highest CH_4 mole fractions also exhibit very low wind speed (0–7 m s^{-1}), indicating formation of nighttime inversion in the atmospheric boundary layer. Stable boundary conditions reduce the mixing volume of emissions, which leads to a stronger CH_4-signal. Variations in the δ^{13}C- and δD-CH_4 values display a clear anti-correlation with the mole fraction changes indicating emissions of CH_4 depleted in $^{13}CH_4$ and CH_3D. The compatibility of different techniques for CH_4 isotopic analysis in ambient air is discussed based on correlation diagrams in the next section.

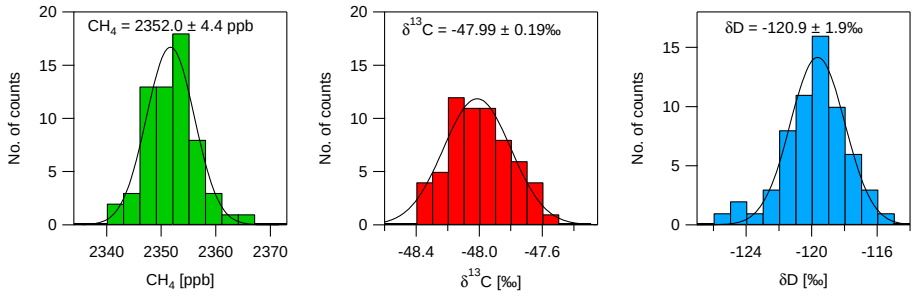

Figure 9. Repeated measurements of pressurized air (target gas) by TREX–QCLAS over 2 weeks throughout the interlaboratory comparison campaign. CH_4 mole fractions and relative differences of isotope ratios (δ^{13}C, δD) were plotted as a histogram with bin widths of 3 ppb (CH_4), 0.1 ‰ (δ^{13}C) and 1 ‰ (δD), respectively. The uncertainty is given as the 1 σ standard deviation.

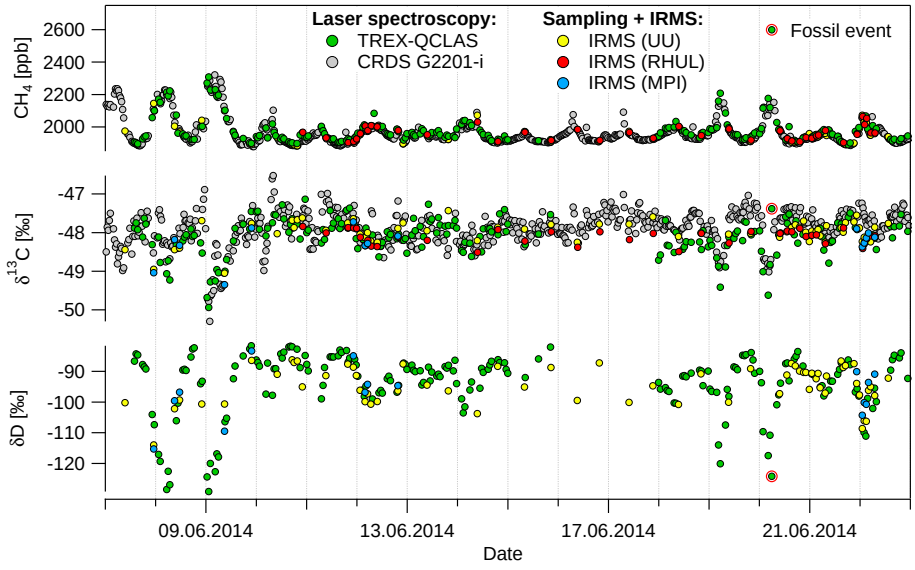

Figure 10. CH_4 mole fractions and isotopic composition analyzed during the interlaboratory comparison campaign in real time by the laser spectroscopic techniques: TREX–QCLAS (CH_4, δ^{13}C, δD), CRDS G2201-i (CH_4, δ^{13}C), and on glass flask/bag samples with IRMS by UU (CH_4, δ^{13}C, δD), MPI (CH_4, δ^{13}C, δD) and RHUL (CH_4, δ^{13}C).

3.4 Compatibility of analytical techniques for δ^{13}C- and δD-CH_4 in ambient air

The compatibility of different analytical techniques for CH_4 isotope measurements was assessed on the ambient air measurements shown in Fig. 10. Measurements were done either on identical gas samples, i.e., for IRMS measurements of glass flask samples by UU and MPI, or on simultaneously collected ambient air samples, i.e., for all other techniques (laser spectrometers and bag samples/IRMS). The δ^{13}C- and δD-CH_4 measurements on glass flasks by IRMS at UU were chosen as reference for this comparison, due to the much higher number of samples ($n = 67$) analyzed as compared to MPI ($n = 15$). Isotope data of all techniques were offset-corrected as described in Sect. 3.2 to account for systematic differences (scale differences and instrumental artifacts) between individual laboratory results.

Figure 11 displays correlation diagrams for the different analytical techniques and laboratories. They exhibit a generally good compatibility of individual techniques. The standard deviation of differences in δ^{13}C-CH_4 values is lowest for the two IRMS techniques that also measured identical samples, intermediate for TREX–QCLAS vs. IRMS and highest for CRDS vs. IRMS, the same order as observed for the repeatability of techniques. Noticeable is also, that the CRDS seems to drift away during certain periods, i.e., on the 18 and 19 June, making the compatibility worse. For δD-CH_4 the standard deviation of differences between TREX–QCLAS and the UU IRMS is comparable or smaller than the one corresponding to the two IRMS systems (UU and MPI), which is also in agreement with repeatability results.

Systematic differences in the δ^{13}C-CH_4 values of individual techniques are small (-0.13 to $+0.2$ ‰) within their extended uncertainties. For δD-CH_4 a similar picture arises

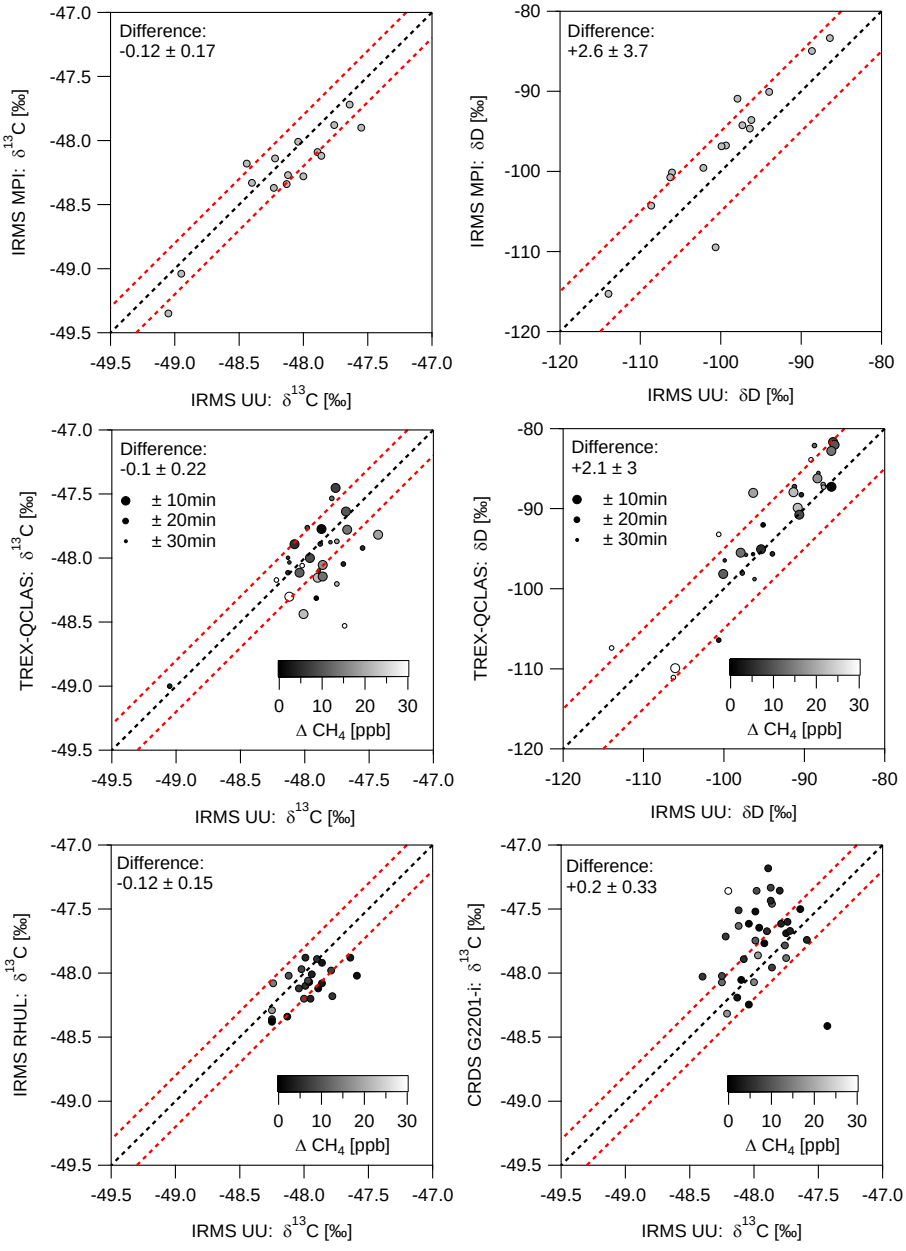

Figure 11. Correlation diagrams for CH_4 isotope (δ^{13}C, δD-CH_4) measurements in ambient air by different techniques and laboratories. The dashed black line is the 1 : 1 line, the red dashed lines indicate the WMO compatibility goals of ± 0.2 ‰ for δ^{13}C and ± 5 ‰ for δD. Results of individual techniques are corrected to a common scale based on MPI results for a pressurized air target gas. For the middle and bottom graphs differences in CH_4 mole fractions in gas samples are represented by the shading (black: identical mole fractions, white: 30 ppb difference). Top: IRMS analysis on glass flasks by the Stable Isotope Laboratory of MPI vs. UU for δ^{13}C-CH_4 (left) and δD-CH_4 (right); Middle: TREX–QCLAS analysis by Empa vs. IRMS analysis on glass flasks by UU for δ^{13}C-CH_4 (left) and δD-CH_4 (right). The temporal difference between TREX–QCLAS analysis and glass flask sampling is indicated by the point size (big: ±10 min, medium: ±20 min, small: ±30 min); Bottom: IRMS analysis on bag samples by RHUL (left) and CRDS analysis by Eawag (right) vs. IRMS analysis on glass flasks by UU for δ^{13}C-CH_4.

with a 2.1 to 2.6 ‰ difference between the applied analytical techniques. These differences in IRMS results of Utrecht University have been introduced by a −2.3 ‰ offset correction based on analysis of the target gas. In summary, the applied offset correction based on the pressurized air target gas led to a consistent data set but also indicates limitations of this correction procedure based on a single gas. This underlines the need for a set of common CH_4 isotope stan-

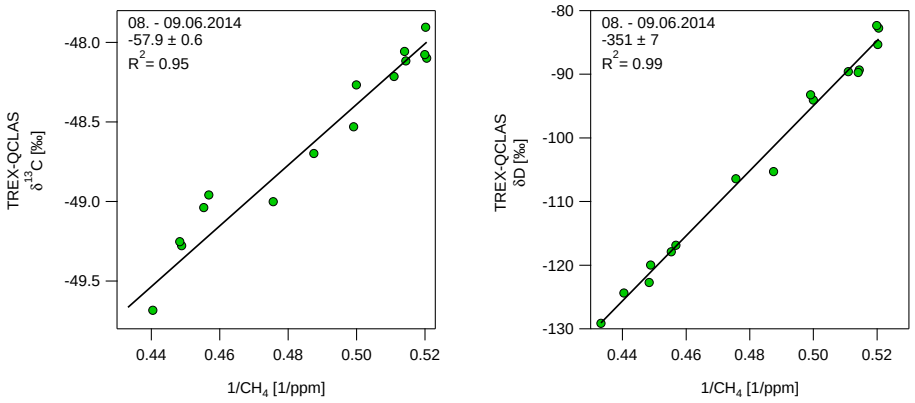

Figure 12. Representative Keeling plots for δ^{13}C-CH_4 and δD-CH_4 for the period 8 June noon till 9 June 2014 noon. The isotopic source signature indicates a microbial origin, possibly referring to CH_4 emissions from ruminants.

dard gases at ambient mole fraction to guarantee the compatibility among different analytical techniques and laboratories. The compatibility of individual techniques with separate sampling is shown in Fig. 11. Deviations in CH_4 mole fractions as well as temporal offsets are illustrated by different shades and symbol sizes, respectively.

3.5 Feasibility of TREX–QCLAS for CH_4 source identification

Keeling plots (Keeling, 1958, 1961) of selected data were used to assess the feasibility of the developed TREX–QCLAS technique for real-time analysis of CH_4 isotopic composition in ambient air and subsequent source appointment (Fig. 12 and Table 3). The data were split into noon-to-noon periods and evaluated when nighttime CH_4 mole fractions exceeded 2050 ppb. By this approach, periods with minor diurnal changes in CH_4 mole fractions were excluded because the derived isotope source signatures have larger uncertainties for small mole fraction elevations. The Keeling plot approach assumes mixing of unpolluted background air with CH_4 from a single source process or a constant mixture of different source processes for one noon-to-noon period. This assumption is valid for most noon-to-noon periods, as indicated by the linear regression parameters (R^2-values) being between 0.63 and 0.95 for δ^{13}C and between 0.97 and 0.99 for δD-CH_4. The period from 19 to 20 June exhibited a low correlation ($R^2\delta^{13}$C : 0.02, δD-CH_4 : 0.85), caused by the contribution of various CH_4 sources as discussed in the next paragraph.

In Fig. 13, CH_4 isotopic source signatures for selected noon-to-noon periods are displayed. All source signatures indicate a major contribution of a microbial CH_4 source process, e.g., by ruminants (Rigby et al., 2012), except the data recorded between 19 and 20 June. During this period there was a singular and pronounced emission event, with CH_4 mole fractions up to 2599 ppb, suggesting significant contributions of CH_4 emissions from a local fossil gas source

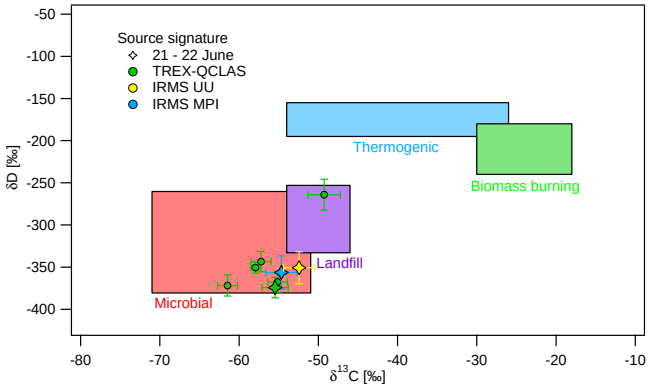

Figure 13. δD-CH_4 vs. δ^{13}C-CH_4 of different CH_4 sources. The symbols indicate CH_4 source signatures derived from Keeling plots. The error bars are uncertainties derived from the linear regression. The star-symbols are source signatures from 21 June noon till 22 June noon derived from different techniques. The shadings indicate typical values for different source categories from the literature.

process. This short lasting (10–20 min) CH_4 emission event was also confirmed by measurements at the nearby monitoring station of the Swiss National Air Pollution Monitoring Network (NABEL), showing a sudden increase in CH_4 mole fractions above 3000 ppb. Using a simple mass balance calculation and clean background air with 1900 ± 15 ppb CH_4 with isotopic composition of -47.5 ‰ for δ^{13}C and -81 ‰ for δD-CH_4 as reported by Bergamaschi et al. (2000), it is rather straightforward to estimate the isotopic signature of this singular event. Thus, the measured values are best explained by an emission source enriched in $^{13}CH_4$ and CH_3D ($\sim -37.2 \pm 1.5$ ‰ for δ^{13}C and $\sim -152 \pm 11$ ‰ for δD) contributing up to 60 % to the observed increase in the CH_4 mole fraction. The remaining 40 % is attributed to microbial sources with isotopic signatures repeatedly determined during the campaign, i.e., -61.5 ‰ for δ^{13}C and -372 ‰ for

Table 3. Overview of all the δ^{13}C-CH_4 and δD-CH_4 source signatures derived using the Keeling plot approach for the given time periods.

System	Time period (12:00–12:00)	#Points	CH_4^{Max}[ppb]	δ^{13}C-CH_4[‰]	δD-CH_4[‰]	R^2-δ^{13}C	R^2-δD
TREX–QCLAS	7–8 Jun 2014	18	2222	-55.1 ± 1.2	-368 ± 13	0.72	0.97
CRDS	7–8 Jun 2014	35	2228	-50.2 ± 0.9		0.16	
TREX–QCLAS	8–9 Jun 2014	18	2308	-57.9 ± 0.6	-351 ± 7	0.95	0.99
CRDS	8–9 Jun 2014	35	2321	-58.8 ± 1.3		0.64	
TREX–QCLAS	18–19 Jun 2014	18	2208	-57.2 ± 1.3	-344 ± 12	0.78	0.97
CRDS	18–19 Jun 2014	35	2147	-58.7 ± 1.0		0.78	
TREX–QCLAS	19–20 Jun 2014[a]	17	2599	-49.7 ± 2.1	-264 ± 18	0.02	0.85
TREX–QCLAS	19–20 Jun 2014[b]	16	2176	-61.5 ± 1.3	-372 ± 12	0.89	0.97
CRDS	19–20 Jun 2014	35	2151	-60.2 ± 1.3		0.74	
TREX–QCLAS	21–22 Jun 2014	15	2067	-55.4 ± 1.7	-374 ± 12	0.63	0.98
IRMS UU	21–22 Jun 2014	10	2072	-52.4 ± 1.9	-351 ± 19	0.34	0.94
IRMS MPI	21–22 Jun 2014	6	2072	-54.7 ± 1.9	-356 ± 20	0.74	0.98
CRDS	22–23 Jun 2014	37	2092	-55.5 ± 0.8		0.71	

Values from the period between 19 and 20 June were derived with [a] and without [b] consideration of the event data point.

δD-CH_4 (see also Table 3). Although, the estimated source signature values agree with fossil origin, it should be noted that the analysis relies only on a single data point. This result, however, is plausible, as no landfill site is situated in the vicinity of the sampling location. When ignoring this emission event, the source signature indicates a microbial source similar to those in other periods (Table 3). Unfortunately, the CRDS analyzer was in calibration mode during this event, and no flask or bag sample was collected for IRMS analysis. This event also highlights the importance of real-time CH_4 isotope analysis. For the period between 21 and 22 June, source signatures obtained by TREX–QCLAS were compared to the IRMS results by UU and MPI of glass flask sampling and the agreement is within the expanded uncertainty of the linear regression (Table 3). Source signatures derived from the CRDS data display a high temporal coverage, but only in four cases the Keeling plot regression analysis lead to reasonable correlations ($R^2 > 0.5$) and thus meaningful source estimates. For all other cases with R^2 below 0.5, the CRDS based signatures deviate significantly from the TREX–QCLAS and IRMS results. In the context of the present study, the increased temporal coverage alone does not provide any additional information, while the unavailability of δD information is a serious limitation with respect to the interpretation of the data.

The measurements made during this campaign clearly demonstrate that the TREX–QCLAS technique is a valuable attractive alternative to the existing laboratory-based techniques that rely on flask sampling. Moreover, the TREX–QCLAS is capable to resolve temporal changes in ambient CH_4 isotopic composition. Finally, the preconcentration unit can be applied for the analysis of mole fraction and isotopic composition of other trace gases, e.g., N_2O and VOCs. The potential of this technique for N_2O isotopes was recently demonstrated in an extended field campaign (Wolf et al., 2015).

4 Conclusion and outlook

This study presents the development and validation of a novel measurement technique, called TREX–QCLAS, for real-time analysis of the three main CH_4 isotopologues $^{12}CH_4$, $^{13}CH_4$ and $^{12}CH_3D$ in ambient air. The fully automated instrument is based on cryogen-free CH_4 preconcentration, followed by selective and high-precision isotope analysis with mid-IR QCL absorption spectroscopy.

This is the first demonstration of analyzing δ^{13}C and δD-CH_4 simultaneously with one instrument in ambient air, real-time and under field conditions. The TREX–QCLAS technique was deployed in an interlaboratory comparison campaign for a period of 2 weeks. Data of the TREX–QCLAS instrument was compared to commercial laser spectroscopic techniques (CRDS, OA–ICOS) as well as to the established IRMS technique using flask or bag sampling. During this period, the TREX–QCLAS performed more than 250 measurement cycles, while 120 air samples were manually collected for subsequent IRMS analysis. The repeatability of TREX–QCLAS based on target gas measurements was found to be 0.19 ‰ for δ^{13}C-CH_4 and 1.9 ‰ for δD-CH_4, which is similar or slightly worse than the state-of-the-art IRMS techniques. Selected noon-to-noon periods of the recorded time-series were analyzed using Keeling plots. During these intervals, the TREX–QCLAS method was able to successfully distinguish between CH_4 emissions with predominantly microbial origin and a case with significant influences from a fossil source.

The intercomparison campaign also exposed calibration scale issues and underlined the need for CH_4 isotope standard gases at ambient mole fractions to improve the com-

patibility among different analytical techniques and laboratories. With its compactness and ability to analyze simultaneously δ^{13}C-CH_4 and δD-CH_4 in a stand-alone operation, the TREX–QCLAS is perfectly suited for field studies at ecosystem measurement sites in order to identify regional source processes.

Acknowledgements. Funding from the Swiss National Science Foundation (SNSF) within grant No. 200021_134611 and the European Community's Seventh Framework Programme (FP7/2007-2013) within the InGOS project under grant agreement No 284274 is gratefully acknowledged. We thank Biogas Volketswil for providing us with pure biogenic CH_4. S. Eyer is very thankful for the continuous support from the electronic (W. Knecht and A. Kunz) and mechanic (U. Hintermüller and E. Pieper) workshops at Empa. In addition we would like to thank Kerstin Zeyer, Antoine Roth and Marco Weber (Empa) for their support. M. E. Popa's travel to Dübendorf was supported by the COST ACTION MP1204 TERA-MIR.

Edited by: M. Hamilton

References

Beck, V., Chen, H., Gerbig, C., Bergamaschi, P., Bruhwiler, L., Houweling, S., Röckmann, T., Kolle, O., Steinbach, J., Koch, T., Sapart, C. J., Van Der Veen, C., Frankenberg, C., Andreae, M. O., Artaxo, P., Longo, K. M., and Wofsy, S. C.: Methane airborne measurements and comparison to global models during BARCA, J. Geophys. Res. Atmos., 117, D15310, doi:10.1029/2011JD017345, 2012.

Bergamaschi, P., Schupp, M., and Harris, G. W.: High-precision direct measurements of $^{13}CH_4/^{12}CH_4$ and $^{12}CH_3D/^{12}CH_4$ ratios in atmospheric methane sources by means of a long-path tunable diode laser absorption spectro, Appl. Opt., 33, 7704–7716, doi:10.1364/AO.33.007704, 1994.

Bergamaschi, P., Brenninkmeijer, C. a. M., Hahn, M., Röckmann, T., Scharffe, D. H., Crutzen, P. J., Elansky, N. F., Belikov, I. B., Trivett, N. B. a., and Worthy, D. E. J.: Isotope analysis based source identification for atmospheric CH_4 and CO sampled across Russia using the Trans-Siberian railroad, J. Geophys. Res., 103, 8227–8235, doi:10.1029/97JD03738, 1998a.

Bergamaschi, P., Lubina, C., Königstedt, R., Fischer, H., Veltkamp, A. C., and Zwaagstra, O.: Stable isotopic signatures (δ^{13}C , δD) of methane from European landfill sites, J. Geophys. Res., 103, 8251–8265, doi:10.1029/98JD00105, 1998b.

Bock, M., Schmitt, J., Behrens, M., Möller, L., Schneider, R., Sapart, C., and Fischer, H.: A gas chromatography/pyrolysis/isotope ratio mass spectrometry system for high-precision δD measurements of atmospheric methane extracted from ice cores, Rapid Commun. Mass Spectrom., 24, 621–633, doi:10.1002/rcm.4429, 2010.

Bock, M., Schmitt, J., Beck, J., Schneider, R., and Fischer, H.: Improving accuracy and precision of ice core δD(CH_4) analyses using methane pre-pyrolysis and hydrogen post-pyrolysis trapping and subsequent chromatographic separation, Atmos. Meas. Tech., 7, 1999–2012, doi:10.5194/amt-7-1999-2014, 2014.

Brand, W. A.: PreCon: A Fully Automated Interface for the Pre-GC Concentration of Trace Gases on Air for Isotopic Analysis, Isotopes Environ. Health Stud., 31, 277–284, doi:10.1080/10256019508036271, 1995.

Brand, W. A. and Coplen, T. B.: Stable isotope deltas: tiny, yet robust signatures in nature, Isotopes Environ. Health Stud., 48, 393–409, doi:10.1080/10256016.2012.666977, 2012.

Brass, M. and Röckmann, T.: Continuous-flow isotope ratio mass spectrometry method for carbon and hydrogen isotope measurements on atmospheric methane, Atmos. Meas. Tech., 3, 1707–1721, doi:10.5194/amt-3-1707-2010, 2010.

Ciais, P., Sabine, C., Bala, G., Bopp, L., Brovkin, V., Canadell, J., Chhabra, A., DeFries, R., Galloway, J., Heimann, M., Jones, C., Le Quéré, C., Myneni, R.B., Piao, S. and Thornton, P.: Carbon and Other Biogeochemical Cycles, in: Climate Change 2013: The Physical Science Basis. Contribution of Working Group I to the Fifth Assessment Report of the Intergovernmental Panel on Climate Change, edited by: Stocker, T. F., Qin, D. , Plattner, G.-K., Tignor, M., Allen, S. K., Boschung, J., Nauels, A., Xia, Y., Bex, V., and Midgley, P. M., Cambridge University Press, Cambridge, UK and New York, NY, USA, 465–570, 2013.

Coplen, T. B.: Guidelines and recommended terms for expression of stable-isotope-ratio and gas-ratio measurement results., Rapid Commun. Mass Spectrom., 25, 2538–2560, doi:10.1002/rcm.5129, 2011.

Curl, R. F., Capasso, F., Gmachl, C., Kosterev, A. A., McManus, J. B., Lewicki, R., Pusharsky, M., Wysocki, G., and Tittel, F. K.: Quantum cascade lasers in chemical physics, Chem. Phys. Lett., 487, 1–18, doi:10.1016/j.cplett.2009.12.073, 2010.

Deans, D. R.: A new technique for heart cutting in gas chromatography [1], Chromatographia, 1, 18–22, doi:10.1007/BF02259005, 1968.

Dlugokencky, E. J., Myers, R. C., Lang, P. M., Masarie, K. A., Crotwell, A. M., Thoning, K. W., Hall, B. D., Elkins, J. W., and Steele, L. P.: Conversion of NOAA atmospheric dry air CH_4 mole fractions to a gravimetrically prepared standard scale, J. Geophys. Res.-Atmos., 110, D18306, doi:10.1029/2005JD006035, 2005.

Dlugokencky, E. J., Nisbet, E. G., Fisher, R., and Lowry, D.: Global atmospheric methane: budget, changes and dangers., Philos. Trans. A. Math. Phys. Eng. Sci., 369, 2058–2072, doi:10.1098/rsta.2010.0341, 2011.

Eyer, S., Stadie, N. P., Borgschulte, A., Emmenegger, L., and Mohn, J.: Methane preconcentration by adsorption: a methodology for materials and conditions selection, Adsorption, 20, 657–666, doi:10.1007/s10450-014-9609-9, 2014.

Faist, J.: Continuous-Wave, Room-Temperature Quantum Cascade Lasers, Opt. Photonics News, 17, 32–36, doi:10.1364/OPN.17.5.000032, 2006.

Faist, K., Hofstetter, D., Beck, M., Aellen, T., Rochat, M., and Blaser, S.: Bound-to-continuum and two-phonon resonance, quantum-cascade lasers for high duty cycle, high-temperature operation, IEEE J. Quantum Electron., 38, 533–546, doi:10.1109/JQE.2002.1005404, 2002.

Fischer, H., Behrens, M., Bock, M., Richter, U., Schmitt, J., Loulergue, L., Chappellaz, J., Spahni, R., Blunier, T., Leuenberger, M., and Stocker, T. F.: Changing boreal methane sources and constant biomass burning during the last termination, Nature, 452, 864–867, doi:10.1038/nature06825, 2008.

Fisher, R., Lowry, D., Wilkin, O., Sriskantharajah, S., and Nisbet, E. G.: High-precision, automated stable isotope analysis of atmospheric methane and carbon dioxide using continuous-flow isotope-ratio mass spectrometry, Rapid Commun. Mass Spectrom., 20, 200–208, doi:10.1002/rcm.2300, 2006.

Keeling, C. D.: The concentration and isotopic abundances of atmospheric carbon dioxide in rural areas, Geochim. Cosmochim. Acta, 13, 322–334, doi:10.1016/0016-7037(58)90033-4, 1958.

Keeling, C. D.: The concentration and isotopic abundances of carbon dioxide in rural and marine air, Geochim. Cosmochim. Acta, 24, 277–298, doi:10.1016/0016-7037(61)90023-0, 1961.

Köster, J. R., Well, R., Tuzson, B., Bol, R., Dittert, K., Giesemann, A., Emmenegger, L., Manninen, A., Cárdenas, L., and Mohn, J.: Novel laser spectroscopic technique for continuous analysis of N_2O isotopomers – application and intercomparison with isotope ratio mass spectrometry, Rapid Commun. Mass Spectrom., 27, 216–222, doi:10.1002/rcm.6434, 2013.

Lowe, D. C., Koshy, K., Bromley, T., Allan, W., Struthers, H., Mani, F., and Maata, M.: Seasonal cycles of mixing ratio and ^{13}C in atmospheric methane at Suva, Fiji, J. Geophys. Res. Atmos., 109, D23308, doi:10.1029/2004JD005166, 2004.

MacFarling Meure, C., Etheridge, D., Trudinger, C., Steele, P., Langenfelds, R., van Ommen, T., Smith, A., and Elkins, J.: Law Dome CO_2 , CH_4 and N_2O ice core records extended to 2000 years BP, Geophys. Res. Lett., 33, L14810, doi:10.1029/2006GL026152, 2006.

Manning, A. C., Nisbet, E. G., Keeling, R. F., and Liss, P. S.: Greenhouse gases in the Earth system: setting the agenda to 2030, Philos. Trans. A. Math. Phys. Eng. Sci., 369, 1885–1890, doi:10.1098/rsta.2011.0076, 2011.

McManus, J. B., Zahniser, M. S., Nelson, D. D., Shorter, J. H., Herndon, S., Wood, E., and Wehr, R.: Application of quantum cascade lasers to high-precision atmospheric trace gas measurements, Opt. Eng., 49, 111124, doi:10.1117/1.3498782, 2010.

McManus, J. B., Zahniser, M. S., and Nelson, D. D.: Dual quantum cascade laser trace gas instrument with astigmatic Herriott cell at high pass number, Appl. Opt., 50, A74–A85, doi:10.1364/AO.50.000A74, 2011.

Miller, B. R., Weiss, R. F., Salameh, P. K., Tanhua, T., Greally, B. R., Mühle, J., and Simmonds, P. G.: Medusa: A sample preconcentration and GC/MS detector system for in situ measurements of atmospheric trace halocarbons, hydrocarbons, and sulfur compounds, Anal. Chem., 80, 1536–1545, doi:10.1021/ac702084k, 2008.

Mohn, J., Guggenheim, C., Tuzson, B., Vollmer, M. K., Toyoda, S., Yoshida, N., and Emmenegger, L.: A liquid nitrogen-free preconcentration unit for measurements of ambient N_2O isotopomers by QCLAS, Atmos. Meas. Tech., 3, 609–618, doi:10.5194/amt-3-609-2010, 2010.

Mohn, J., Tuzson, B., Manninen, A., Yoshida, N., Toyoda, S., Brand, W. A., and Emmenegger, L.: Site selective real-time measurements of atmospheric N_2O isotopomers by laser spectroscopy, Atmos. Meas. Tech., 5, 1601–1609, doi:10.5194/amt-5-1601-2012, 2012.

Mohn, J., Steinlin, C., Merbold, L., Emmenegger, L., and Hagedorn, F.: N_2O emissions and source processes in snow-covered soils in the Swiss Alps, Isotopes Environ. Health Stud., 49, 520–531, doi:10.1080/10256016.2013.826212, 2013.

Mohn, J., Wolf, B., Toyoda, S., Lin, C.-T., Liang, M.-C., Brüggemann, N., Wissel, H., Steiker, A. E., Dyckmans, J., Szwec, L., Ostrom, N. E., Casciotti, K. L., Forbes, M., Giesemann, A., Well, R., Doucett, R. R., Yarnes, C. T., Ridley, A. R., Kaiser, J., and Yoshida, N.: Interlaboratory assessment of nitrous oxide isotopomer analysis by isotope ratio mass spectrometry and laser spectroscopy: current status and perspectives, Rapid Commun. Mass Spectrom., 28, 1995–2007, doi:10.1002/rcm.6982, 2014.

Monteil, G., Houweling, S., Dlugockenky, E. J., Maenhout, G., Vaughn, B. H., White, J. W. C., and Rockmann, T.: Interpreting methane variations in the past two decades using measurements of CH_4 mixing ratio and isotopic composition, Atmos. Chem. Phys., 11, 9141–9153, doi:10.5194/acp-11-9141-2011, 2011.

Nisbet, E. G., Dlugokencky, E. J., and Bousquet, P.: Methane on the rise-again, Science, 343, 493–495, doi:10.1126/science.1247828, 2014.

Rigby, M., Manning, a. J., and Prinn, R. G.: The value of high-frequency, high-precision methane isotopologue measurements for source and sink estimation, J. Geophys. Res. Atmos., 117, D12312, doi:10.1029/2011JD017384, 2012.

Santoni, G. W., Lee, B. H., Goodrich, J. P., Varner, R. K., Crill, P. M., McManus, J. B., Nelson, D. D., Zahniser, M. S., and Wofsy, S. C.: Mass fluxes and isofluxes of methane (CH_4) at a New Hampshire fen measured by a continuous wave quantum cascade laser spectrometer, J. Geophys. Res. Atmos., 117, D10301, doi:10.1029/2011JD016960, 2012.

Sapart, C. J., Monteil, G., Prokopiou, M., van de Wal, R. S. W., Kaplan, J. O., Sperlich, P., Krumhardt, K. M., van der Veen, C., Houweling, S., Krol, M. C., Blunier, T., Sowers, T., Martinerie, P., Witrant, E., Dahl-Jensen, D., and Röckmann, T.: Natural and anthropogenic variations in methane sources during the past two millennia, Nature, 490, 85–88, doi:10.1038/nature11461, 2012.

Schmitt, J., Seth, B., Bock, M., van der Veen, C., Möller, L., Sapart, C. J., Prokopiou, M., Sowers, T., Röckmann, T., and Fischer, H.: On the interference of Kr during carbon isotope analysis of methane using continuous-flow combustion-isotope ratio mass spectrometry, Atmos. Meas. Tech., 6, 1425–1445, doi:10.5194/amt-6-1425-2013, 2013.

Schmitt, J., Seth, B., Bock, M., and Fischer, H.: Online technique for isotope and mixing ratios of CH_4, N_2O, Xe and mixing ratios of organic trace gases on a single ice core sample, Atmos. Meas. Tech., 7, 2645–2665, doi:10.5194/amt-7-2645-2014, 2014.

Sperlich, P., Guillevic, M., Buizert, C., Jenk, T. M., Sapart, C. J., Schaefer, H., Popp, T. J., and Blunier, T.: A combustion setup to precisely reference δ^{13}C and δ^{2}H isotope ratios of pure CH_4 to produce isotope reference gases of δ^{13}C-CH_4 in synthetic air, Atmos. Meas. Tech., 5, 2227–2236, doi:10.5194/amt-5-2227-2012, 2012.

Sperlich, P., Buizert, C., Jenk, T. M., Sapart, C. J., Prokopiou, M., Röckmann, T., and Blunier, T.: An automated GC-C-GC-IRMS setup to measure palaeoatmospheric δ^{13}C-CH_4, δ^{15}N-N_2O and δ^{18}O-N_2O in one ice core sample, Atmos. Meas. Tech., 6, 2027–2041, doi:10.5194/amt-6-2027-2013, 2013.

Sturm, P., Tuzson, B., Henne, S., and Emmenegger, L.: Tracking isotopic signatures of CO_2 at the high altitude site Jungfraujoch with laser spectroscopy: analytical improvements and representative results, Atmos. Meas. Tech., 6, 1659–1671, doi:10.5194/amt-6-1659-2013, 2013.

Tuzson, B., Mohn, J., Zeeman, M. J., Werner, R. a., Eugster, W., Zahniser, M. S., Nelson, D. D., McManus, J. B., and Emmenegger, L.: High precision and continuous field measurements of δ^{13}C and δ^{18}O in carbon dioxide with a cryogen-free QCLAS, Appl. Phys. B Lasers Opt., 92, 451–458, doi:10.1007/s00340-008-3085-4, 2008.

Tuzson, B., Hiller, R. V., Zeyer, K., Eugster, W., Neftel, A., Ammann, C., and Emmenegger, L.: Field intercomparison of two optical analyzers for CH_4 eddy covariance flux measurements, Atmos. Meas. Tech., 3, 1519–1531, doi:10.5194/amt-3-1519-2010, 2010.

Urey, H. C.: Oxygen Isotopes in Nature and in the Laboratory, Science, 108, 489–496, doi:10.1126/science.108.2810.489, 1948.

Waechter, H., Mohn, J., Tuzson, B., Emmenegger, L., and Sigrist, M. W.: Determination of N_2O isotopomers with quantum cascade laser based absorption spectroscopy, Opt. Express, 16, 9239–9244, doi:10.1364/OE.16.009239, 2008.

Werle, P.: Accuracy and precision of laser spectrometers for trace gas sensing in the presence of optical fringes and atmospheric turbulence, Appl. Phys. B, 102, 313–329, doi:10.1007/s00340-010-4165-9, 2010.

Werner, R. A. and Brand, W. a.: Referencing strategies and techniques in stable isotope ratio analysis, Rapid Commun. Mass Spectrom., 15, 501–519, doi:10.1002/rcm.258, 2001.

WMO/GAW: GAW Report No. 213 17th WMO/IAEA Meeting on Carbon Dioxide , Other Greenhouse Gases and Related Tracers Measurement Techniques (GGMT-2013), Beijing, available from: http://www.wmo.int/pages/prog/arep/gaw/gaw-reports.html, last access: 13 June 2013.

WMO/GAW: WMO Greenhouse Gas Bulletin, available at: http://www.wmo.int/pages/prog/arep/gaw/ghg/GHGbulletin.html, last access: 9 November 2015.

Wolf, B., Merbold, L., Decock, C., Tuzson, B., Harris, E., Six, J., Emmenegger, L., and Mohn, J.: First on-line isotopic characterization of N_2O above intensively managed grassland, Biogeosciences, 12, 2517–2531, doi:10.5194/bg-12-2517-2015, 2015.